Ultrastructure of Reichert's Membrane, a Multilayered Basement Membrane in the Parietal Wall of the Rat Yolk Sac

S. INOUÉ, C. P. LEBLOND, and G. W. LAURIE
Department of Anatomy, McGill University, Montreal, Quebec, Canada H3A 2B2

ABSTRACT The ultrastructure of Reichert's membrane, a thick basement membrane in the parietal wall of the yolk sac, has been examined in 13–14-d pregnant rats. This membrane is composed of more or less distinct parallel layers, each one of which resembles a common basement membrane. After routine fixation in glutaraldehyde followed by osmium tetroxide, the layers appear to be mainly composed of 3–8-nm thick cords arranged in a three-dimensional network. Loosely scattered among the cords are unbranched, straight tubular structures with a diameter of 7–10 nm, which mainly run parallel to the surface and to one another; they are referred to as basotubules. Permanganate fixation emphasizes the presence of a thick feltwork of irregular material around basotubules. Finally, minute dot-like structures measuring 3.5 nm and referred to as double pegs are present within the meshes of the cord network.

Reichert's membranes have been treated for 2–48 h at 25°C with plasmin, a proteolytic enzyme known to rapidly digest laminin and fibronectin. After a 2-h treatment, most of the substance of the cords is digested away leaving a three-dimensional network of 1.5–2.0-nm thick filaments. The interpretation is that the cords are formed of a plasmin-resistant core filament and a plasmin-extractable sheath. When plasmin treatment is prolonged for 15 h or longer, the filaments are dissociated and disappear, while basotubules are maintained. Plasmin digestion also reveals that basotubules are composed of two parts: a ribbon-like helical wrapping and tubule proper. Further changes in the tubule under plasmin influence are interpreted as a dissociation into pentagonal units suggestive of the presence of the amyloid P component. After 48 h of plasmin treatment, basotubules are further disaggregated and dispersed, leaving only linearly arranged double pegs.

Reichert's membranes with or without a 2-hr plasmin treatment have been immunostained by exposure to antibodies against either laminin or type IV collagen with the help of peroxidase markers. The results indicate that the sheath of the cords contains laminin antigenicity, while the core filament contains type IV collagen antigenicity.

It is proposed that Reichert's membrane consists mainly of a three-dimensional network of cords composed of a type IV collagen filament enclosed within a laminin-containing sheath. Also present are basotubules—which may contain the amyloid P component—and double pegs whose nature is unknown.

Basement membrane is a thin matrix that separates connective tissue from epithelial, endothelial, fat, and muscle cells, and also from the nervous system. The electron microscope shows that basement membranes commonly are composed of three layers. The two main ones are the 10–50-nm thick lamina lucida (also called rara) adjacent to the cells and, next to it, the 20–300-nm thick lamina densa (also called basal lamina), while a third, poorly defined layer, the lamina or pars fibroreticularis, makes up the transition with connective tissue[1] (1, 2). Basement membranes are said to be composed

[1] The layers of the basement membrane are described in the terms recently recommended by the International Anatomical Nomenclature Committee as reported in the "Nomina Histologica" section of *Nomina Anatomica* (1983, 5th Edition, Williams and Wilkins, Baltimore, MD), that is lamina lucida, lamina densa, and lamina (pars)

THE JOURNAL OF CELL BIOLOGY · VOLUME 97 NOVEMBER 1983 1524–1537

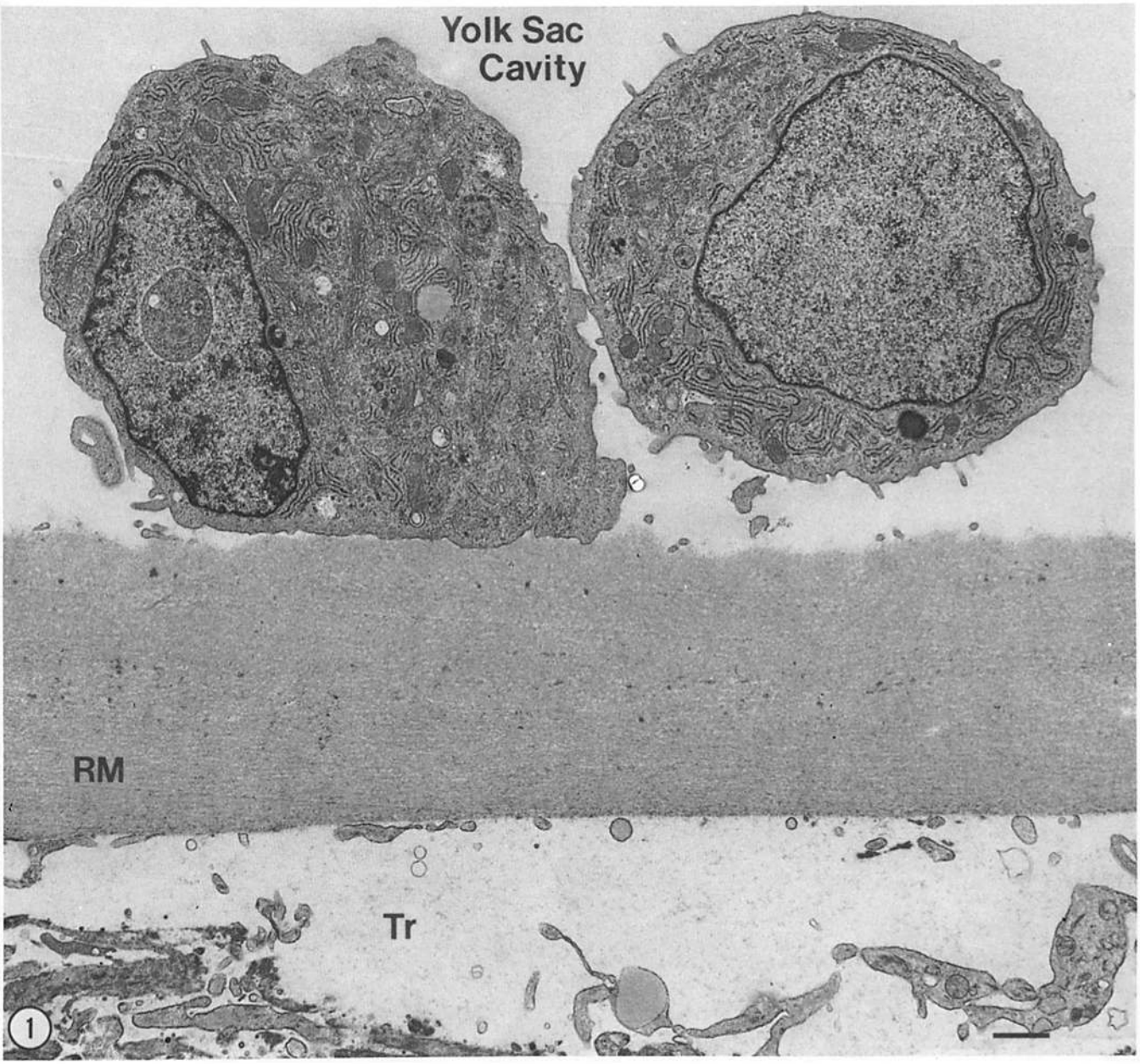

FIGURE 1 Reichert's membrane (*RM*) extends across the figure. Above on the embryo side, two endodermal cells are within the yolk sac cavity, whereas below on the uterine wall side is a blood sinus from the labyrinth portion of the trophoblast (*Tr*). The membrane shows discrete layering. Bar, 1 μm. × 8,600.

of 3–4-nm fibrils in an amorphous ground substance (3–7). An additional type of fibril with a 10-nm diameter and a hollow profile also has been observed in the basement membranes of kidney glomerulus (3, 4, 7). Yet, there has been little systematic investigation of ultrastructure, perhaps because of the difficulty of working with most basement membranes, which are thin and irregularly oriented.

In contrast, Reichert's membrane, the thick basement membrane found in the parietal wall of the rat yolk sac, may be handled for treatment by enzymes or antibodies far more readily than common basement membranes; and it was decided to investigate its ultrastructure. The study was carried out in rats 13–14-d pregnant, since at that time the membrane is close to maximal size and shows no signs of degeneration, unlike what happens in the next few days when the membrane breaks up and disappears. Finally, the membrane at that time is composed of more or less distinct layers stacked in parallel with the surface and resembling superimposed laminae densae (8). Previous reports only indicated that Reichert's membrane was composed of fine fibrils (9–12) 2–8 nm in thickness (8). In the present article, the ultrastructure of Reichert's membrane was examined in three steps. In the first, several structural components were identified after routine or permanganate fixation using sections cut either across Reichert's membrane or parallel to its surface. The second step was suggested by results of Liotta et al (13) indicating that plasmin at 25°C degraded laminin and fibronectin, but had little effect on type

fibroreticularis. We have accordingly replaced the term "basal lamina," which we used previously, by the term "lamina densa." The term "basal lamina" was indeed ambiguous since it was considered by some authors as synonymous with "basement membrane."

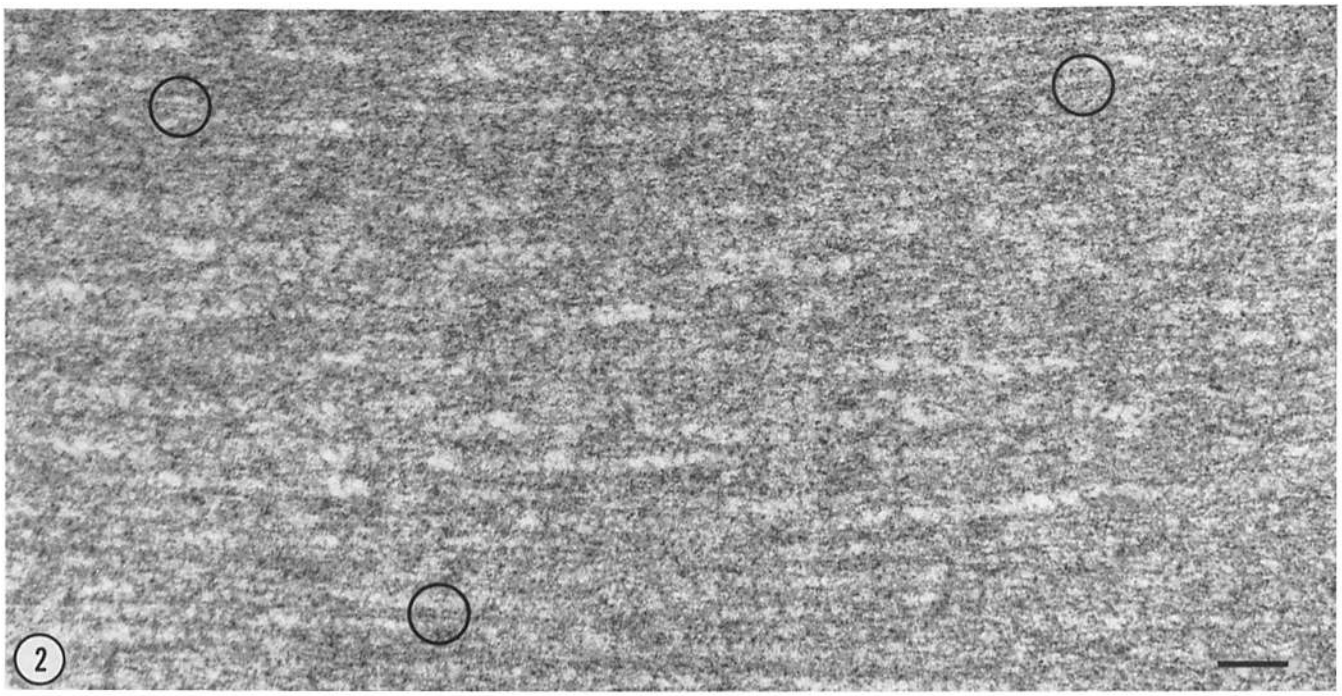
2

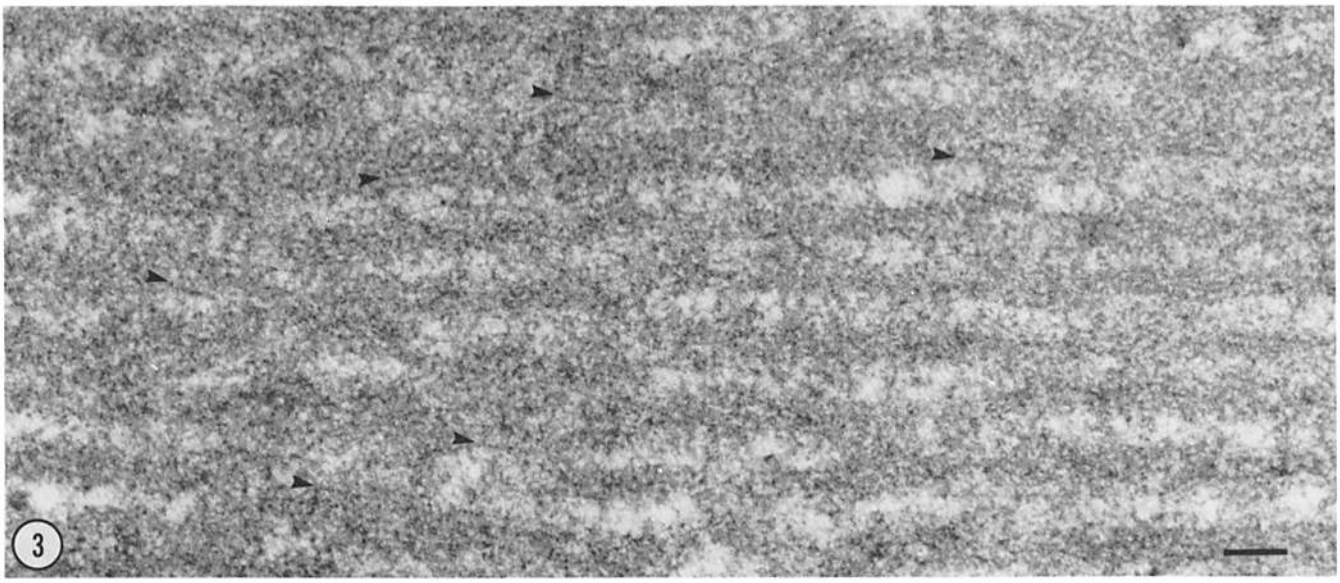
3

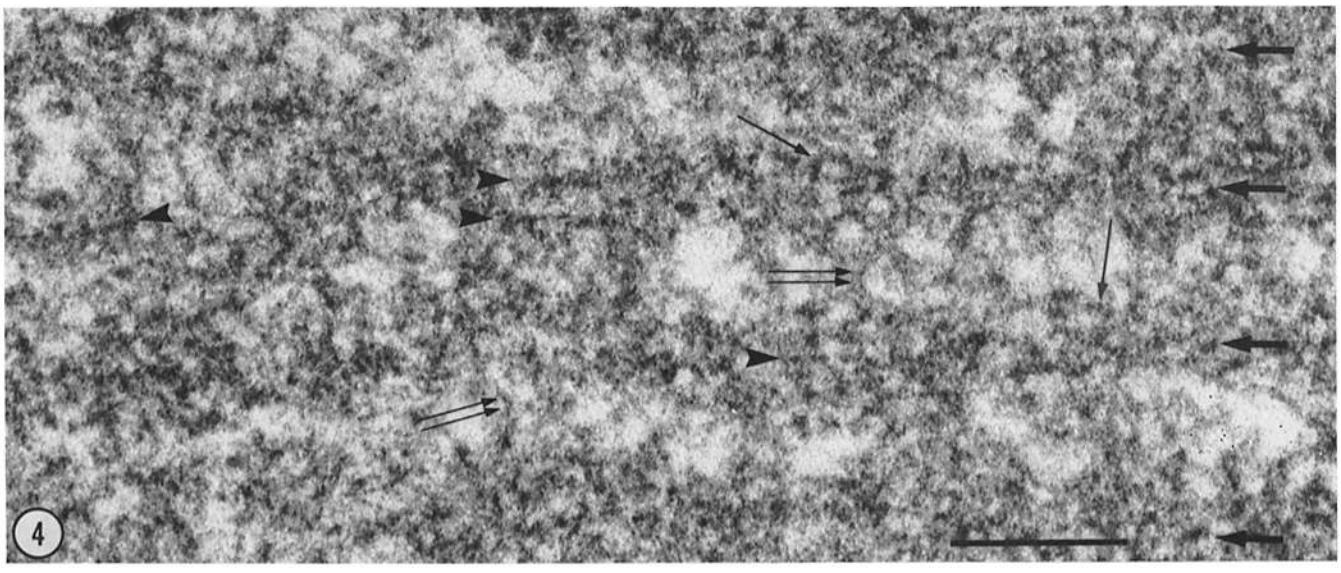
4

IV collagen. Furthermore, these authors reported that treatment of the amniotic basement membrane with plasmin extracted laminin antigenicity, but not type IV collagen antigenicity. Since Reichert's membrane was known to contain laminin (14–17) and type IV collagen (18–20), it was hoped that treatment with plasmin could help in assigning laminin to some of the structural components. In a third stage, immunostaining for laminin and type IV collagen was applied to Reichert's membrane. The results obtained by these three approaches provided a comprehensive survey of Reichert's membrane ultrastructure at 13–14 d of pregnancy.

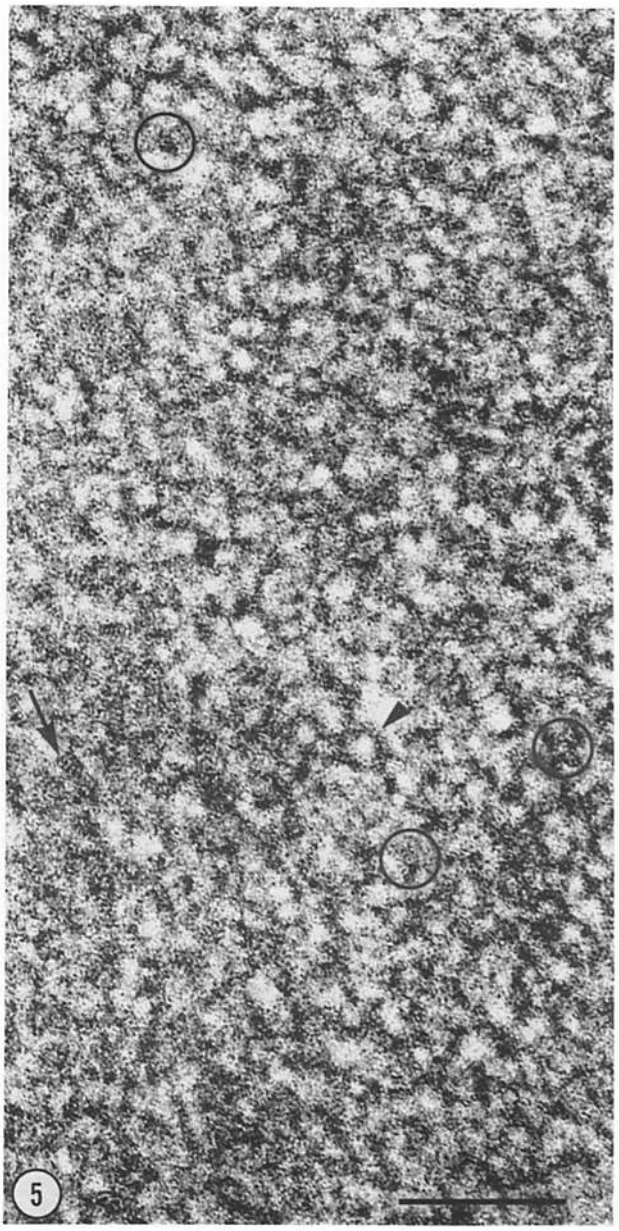

FIGURE 5 Preparation of Reichert's membrane fixed directly in osmium-ferrocyanide and sectioned approximately parallel to the surface. Cords (arrowhead) are arranged in an extensive network and outline light spaces. Some cords show a series of transverse, more or less parallel thread-like elements as may be seen at the arrow and nearby. The few visible basotubles are cut in cross section (circles). Bar, 0.1 μm. × 219,200.

MATERIALS AND METHODS

Ultrastructure of Reichert's Membrane: Female Sherman rats of 13–14 d pregnancy were incised under anesthesia to expose the uterus; and a fixative made up of 3% glutaraldehyde in 0.1 M sodium cacodylate buffer at pH 7.4 was injected into the chorioallantoic placentae of two adjacent concepti and into the uterine lumen nearby (8). Concepti were removed and immersed into fresh fixative for ~20 min. Strips of parietal yolk sac were cut out from the capsular portion under a dissecting microscope, further slit into 1-mm × 2-mm pieces and kept for another 3 h in fresh fixative at room temperature. The pieces were then processed at 4°C, being first washed in several changes of 0.1 M sodium cacodylate buffer, then postfixed in 1% osmium tetroxide in the same buffer for 90 min, stained en block with 2% uranyl acetate for 1 h, and dehydrated in graded series of acetone. For embedding in Epon 812, they were oriented so as to be cut either parallel to the surface or perpendicular to it. Thin sections were stained with uranyl acetate followed by lead citrate for electron microscopy. In addition, strips of parietal yolk sac were postfixed in osmium-potassium ferrocyanide (21). Others were initially fixed in 3% potassium permanganate in glucose-containing Krebs-Henseleit saline solution at 4°C for 30 min and stained en bloc with 1% uranyl acetate for 45 min (22).

The sections were examined in a Philips EM400 electron microscope after calibration of magnification by a catalase crystal standard. For stereo-electron micrographs, the specimens were tilted ± 6°. Size was measured on prints by means of a hand magnifier equipped with a 0.1-mm scale.

Effect of Plasmin: Plasmin treatment by the method of Liotta et al. (13) was carried out directly on parietal yolk sacs dissected from 13–14-d pregnant rats in the cases depicted in Figs. 18–21, or on Reichert's membranes isolated by the method of Clark et al. (9) in the cases illustrated in Figs. 13–17 and 22–23. After either method of isolation, the specimens were washed with PBS at pH 7.4, incubated at 25°C for 2, 15, 24, or 48 h in purified plasmin (kindly provided by Dr. Lance Liotta, National Institutes of Health, Bethesda, MD) and then washed several times in PBS, with care being taken not to disrupt the delicate structure of the digested material. After plasmin treatment, the specimens were fixed at room temperature for 3 h with 3% glutaraldehyde in 0.1 M sodium cacodylate buffer at pH 7.4; they were washed in buffer, postfixed in 1% OsO_4, and processed as described above for electron microscopy.

Immunostaining: Parietal yolk sacs, either untreated or treated for 2 h with plasmin as above, were fixed in 5% formaldehyde for 3 h at 4°C as described elsewhere (20). Specimens were processed whole or after cutting into 60-μm slices using a Smith and Farquhar tissue chopper. They were then incubated overnight at 4°C either with antilaminin antibodies (0.06 mg/ml) or with antitype IV collagen antibodies bound to peroxidase (0.3 mg IgG per ml), followed either by the sequence of peroxidase-antiperoxidase in the case of laminin staining (17) or by extensive washing with PBS in the case of type IV collagen staining (20). The immunostaining was then achieved by passage through diaminobenzidine (DAB)-H_2O_2 for 10 min, followed by osmium tetroxide for 15 min. The tissues were further processed for embedding and thin sectioning for electron microscopy.

The specificity of the antilaminin and antitype IV collagen antibodies (kindly supplied by Dr. George R. Martin, National Institutes of Health, Bethesda, MD) was determined by enzyme-linked immunosorbent assay (ELISA). The antilaminin antibodies were purified in Dr. Martin's laboratories by sequential

FIGURES 2–4 Fig. 2: Section cut perpendicularly to the surface of Reichert's membrane and showing rather thin layers. By chance, several basotubules cut along their length are included; they appear as distinct tubules with electron dense, double walls separated by a lighter lumen (circles). Bar, 0.1 μm. × 91,800. Fig. 3: Section cut perpendicularly to the surface of Reichert's membrane and showing rather thick layers separated by electron lucent spaces. A few obliquely sectioned basotubules are seen as short straight rods (arrowheads). Bar, 0.1 μm. × 83,100. Fig. 4: Higher power view of Reichert's membrane. The layers are highlighted by thick arrows at right. Each layer mainly consists of interconnected strands, referred to as cords (single thin arrows). Cords are also seen extending across the lucent spaces which separate the layers (double thin arrows). Oblique sections of basotubules are indicated by arrowheads. Bar, 0.1 μm. × 228,400.

gen antibodies showed no cross-reactivity by ELISA with other basement membrane components and were used without further purification. Controls were carried out by exposure to nonimmune rabbit serum.

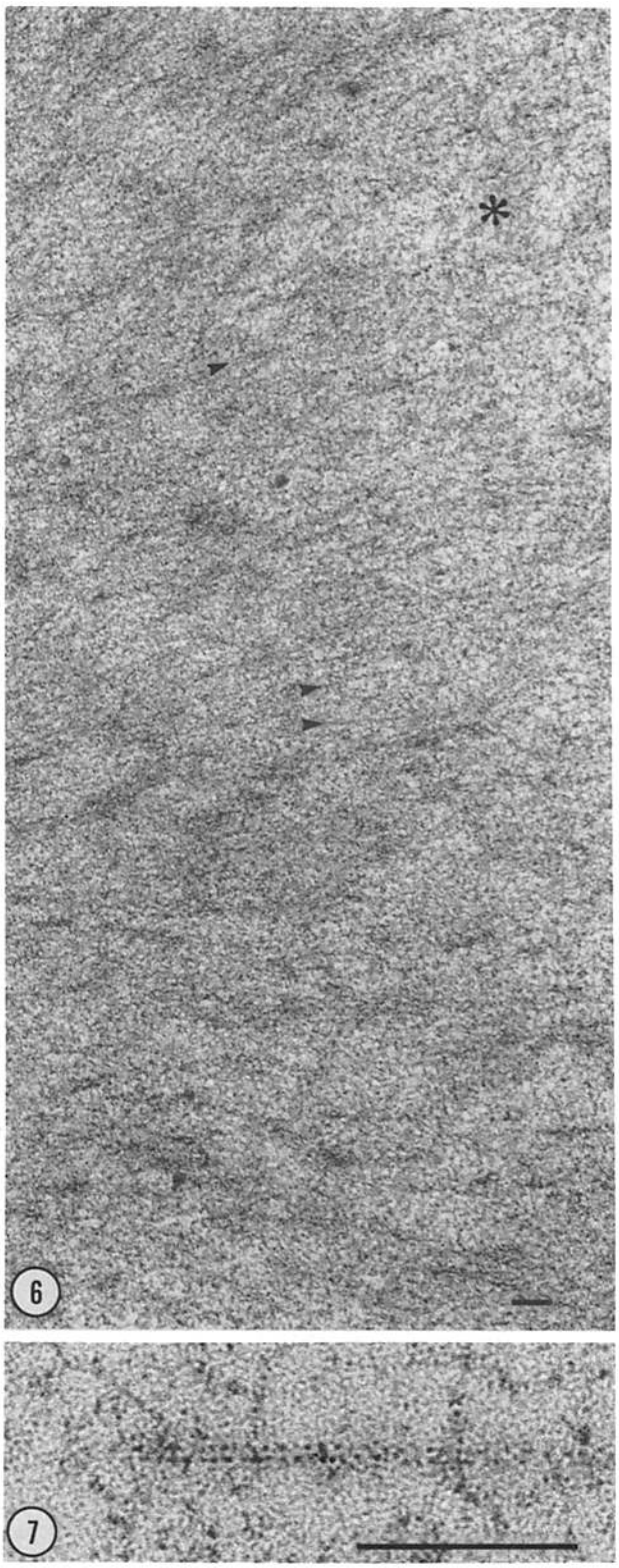

FIGURES 6 and 7 Fig. 6: A layer of Reichert's membrane sectioned parallel to its surface shows numerous basotubules (arrowheads), which seem to radiate from left to right. The network of cords may be faintly distinguished between basotubules (asterisk). Bar, 0.1 μm. × 51,300. Fig. 7: High power view of a basotubule with a 7.5-nm diam. The lumen is visible between the stain-dotted walls. Bar, 0.1 μm. × 288,200.

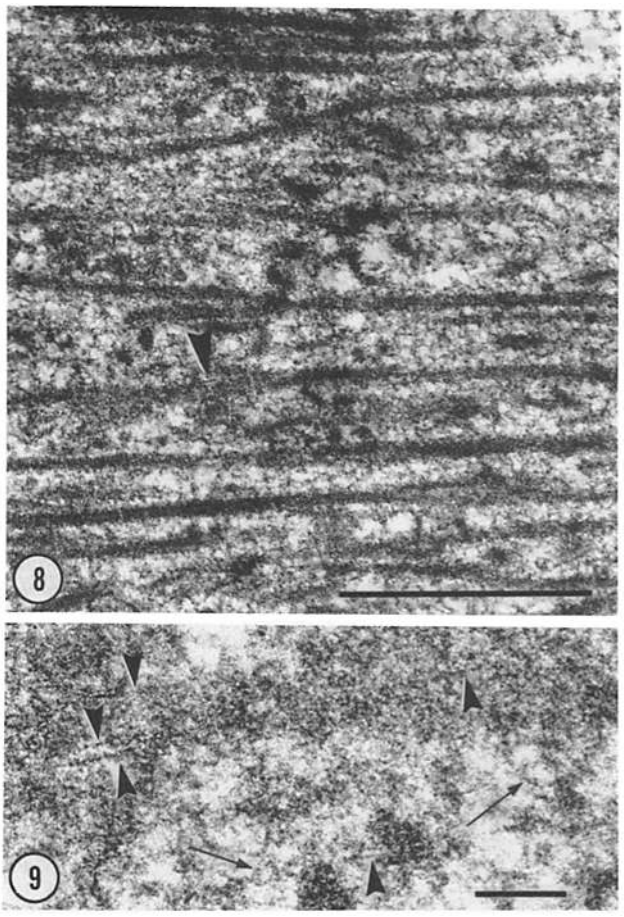

FIGURES 8 and 9 Reichert's membrane fixed in potassium permanganate and stained with uranium-lead. Fig. 8: Dense bars emphasized by permanganate fixation extend across the picture: they are referred to as "peritubular feltwork." Within them, it is occasionally possible to distinguish a fine rod (arrowhead) identified as basotubule. Bar, 1 μm. × 33,700. Fig. 9: Higher power view of a dense bar showing the irregularity of the peritubular feltwork surrounding basotubules (arrowheads). The network of cords is not readily visible after permanganate fixation, but may be distinguished in parts of the figure (arrows). Bar, 0.1 μm. × 119,300.

RESULTS

Ultrastructure of Reichert's Membrane

Reichert's membrane is associated with a layer of endodermal cells on the surface facing the yolk sac cavity and the embryo, and with the fetal sinuses and maternal blood spaces of the trophoblast on the outer surface (Fig. 1).[2] At 13–14 d gestation in the rat, Reichert's membrane is composed of a variable number of more or less distinct superimposed layers that run parallel to the plane of the membrane (Figs. 2 and 3). The layers may be missing in places, but usually ~40 can be distinguished. The thickness of the layers is variable, being ~25 nm in the specimen depicted in Fig. 2 and 50 nm in Fig. 3. The thickness of the lucent interlayer spaces is only about half that of the layers.

At low magnification, the layers seem to be composed of

[2] All figures depict Reichert's membrane from the parietal yolk sac of rats at 13–14 d of pregnancy. Unless otherwise indicated, the specimens have been fixed in glutaraldehyde, postfixed in osmium tetroxide, and stained in uranium and lead for electron microscopy.

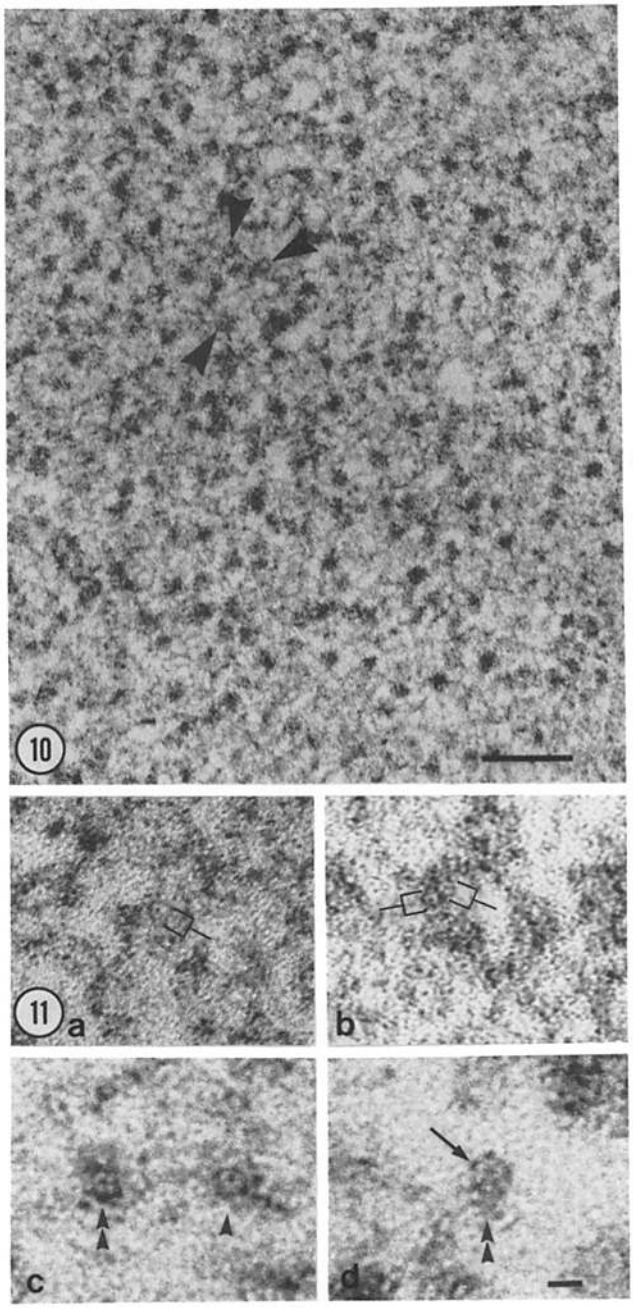

FIGURES 10 and 11 Fig. 10: Cross section of Reichert's membrane fixed in potassium permanganate and stained in uranium-lead. A number of irregular dense spots represent cross sections of peritubular feltwork (less prominently stained than in Fig. 8). Within the peritubular feltwork, cross sections of basotubules may be faintly distinguished (arrowheads). Cords are present, but less prominent than after glutaraldehyde fixation. Bar, 0.1 μm. × 119,600. Fig. 11: Higher power micrographs of cross sections of basotubules. Fig. 11 *a* depicts a glutaraldehyde-fixed specimen, in the center of which can be seen the cross section of a basotuble (indicated by bracket). A dot is in the middle of the cross section. In contrast to permanganate-fixed preparations, the peritubular feltwork is not obvious, but the cord network is prominent.

The other figures represent permanganate-fixed specimens. Cross section of two basotubules surrounded by a prominent peritubular feltwork is shown in Fig. 11 *b*. In *c* and *d*, the cross sections are surrounded by little or no feltwork; their diameter is then enlarged (single arrowheads) and they tend to appear pentagonal rather than circular (double arrowheads). Tiny, electron-dense dots are seen in the center and at the five points of the pentagons in Fig. 14 *d* (arrow). Bar, 0.1 μm. × 443,400.

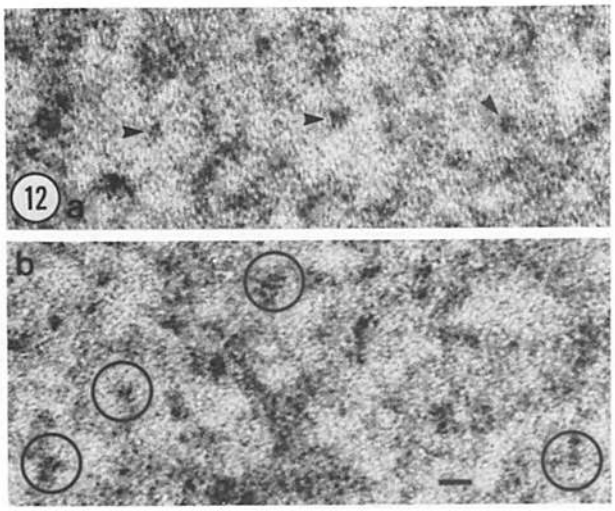

FIGURE 12 High power micrographs of Reichert's membrane. In *a*, minute particulate structures (arrowheads) are seen toward the center of the meshes of the cord network. *b* shows the fine structure of these particles as two short parallel rods (circles). These structures are referred to as double pegs. Bar, 0.1 μm. × 428,500.

material that appears finely granular or fibrillar (Fig. 3), but is seen at high magnification as a network of interconnected "cords" (Fig. 4, thin arrows). In addition, there is a loose scattering of straight rods often seen in oblique sections (arrowheads, Figs. 3 and 4). When these rods are cut along their length, they show a lumen (Fig. 2, circles). They are, therefore, tubular and will be referred to as "basement membrane tubules" or "basotubules."

The cords that constitute the bulk of Reichert's membrane are irregular strands measuring from 3 to 8 nm in thickness, with an average of 5 nm. Cords are densely packed within the layers, but extend in a looser arrangement across the lucent interlayer spaces (Fig. 4). The network arrangement of the cords may be seen in sections parallel to the surface of Reichert's membrane (Fig. 5). Individual cords may show a series of 1.5–2-nm wide transverse thread-like elements (Fig. 5, arrow). The meshes or openings of the network range from 7 to 60 nm with an average of 15 nm.

The basotubules that are loosely scattered in Reichert's membrane are usually located within the plane of a layer where they run parallel to one another or radiate in a fan-like manner (Fig. 6). However, they may also run obliquely to the layers (Fig. 3). Individual basotubules are fairly straight and unbranched (Fig. 7), although the odd curved one has been encountered. Their diameter averages 7 nm, but may on occasion exceed 10 nm. The 3–4-nm lumen may be distinguished at medium magnification (Fig. 2) and is clear-cut at high magnification (Fig. 7).

After fixation in potassium permanganate, the cords are less visible than after glutaraldehyde, while electron-dense, elongated bars become prominent (Fig. 8). The thickness of the bars varies along their length (Fig. 9), but also according to the specimen; thus they are ~60 nm thick in Fig. 8, but only ~20 nm thick in the cross sections shown in Fig. 10. It is not known whether such a difference is real or depends on the amount of permanganate diffusing within Reichert's membrane. Bands have been enumerated in cross sections such as that in Fig. 10 and found to average 360 per μm^2. When a bar is examined at medium or high magnification, it is sometimes possible to distinguish one, two, or more fine rods within it (Fig. 9). In cross section, these fine rods show a

7-nm diameter and a 3–4-nm lumen (Fig. 11, *b*) and, therefore, may be identified as basotubules. The lumen of basotubules contains a 1.3-nm dot, which indicates the presence of either a central filament or a string of dots running along the axis of the tubule. Besides the presence of one, two, or more basotubules, the bars are mainly composed of a variable amount of irregular, dense material, which will be referred to as "peritubular feltwork." Occasionally, there seems to be little or even no peritubular feltwork around a basotubule, in which case the diameter tends to be greater than normally, up to 14 nm, and the outline appears pentagonal rather than circular (Fig. 11, *c* and *d*). The central dot is connected by faint spokes to the sides of the pentagons (Fig. 11 *d*). The basotubules observed in preparations fixed in glutaraldehyde also show a central dot (Fig. 11 *a*), while the peritubular feltwork is less distinct than after permanganate fixation.

Finally, examination of the light spaces separating the cords shows minute particulate structures toward their center (Fig. 12 *a*). They are tentatively referred to as "double pegs" since, when their orientation is favorable, they appear as tiny parallel rods separated by a narrow space (Fig. 12 *b*). Their length and width are estimated at 3.5 nm. It will be shown below that double pegs seem to be strung along very fine filaments.

Effects of Plasmin

When Reichert's membrane was incubated in plasmin, the digestion proceeded slowly, but unevenly. The membrane remained continuous and resilient after a 2-h treatment, but became swollen and fragile after 15 h. By 48 h, the membrane consisted of a fragile jelly-like mass.

CORDS: After a 2-h treatment, an area where the cords are nearly normal may be seen next to another in which they appear denuded and reduced to a filament (Fig. 13). At what appears to be a very early stage in digestion, the cord remnants consist of a filament associated with transverse thread-like elements (Fig. 13, inset) similar to, but less regular than those observed under normal conditions. At a more advanced stage, the thread-like elements disappear, leaving only the axial filament, as seen in the center of Fig. 13. Each filament runs singly, but joins others to form a network that, upon examination of stereopairs, is seen to extend in three dimensions (Fig. 14). Our interpretation is that the cords are composed of a "core filament" enclosed within a "sheath" in which transverse thread-like elements may be observed.

Examination of stereo pairs shows the continuity of the filament network. When sections are examined in three-

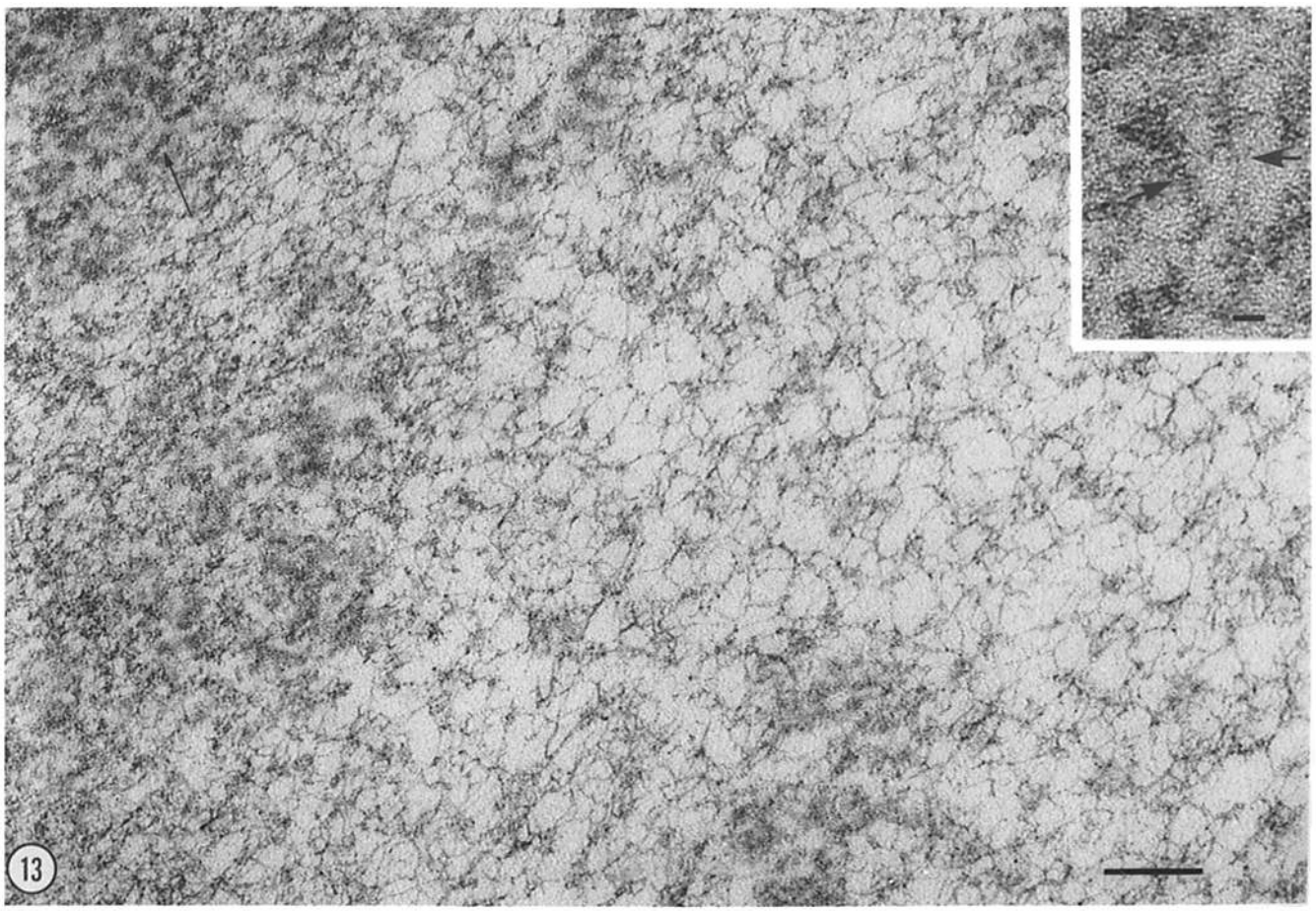

FIGURE 13 Electron micrograph of Reichert's membrane following treatment with plasmin for 2 h and fixation in glutaraldehyde. The left side shows nearly intact cords (arrow), whereas the center depicts a more advanced stage of digestion in which the cord network has been replaced by a network of fine filaments. This is interpreted to mean that plasmin has digested the peripheral sheath of the cords to reveal a fine filament core. Along the filaments, dot-like thickenings are scattered irregularly. Some of them are true dots, while others represent filaments oriented perpendicularly to the section surface. At higher power, the *inset* demonstrates that a fine filament forms the core of a cord. At the arrows, two partially digested cords have their sheath reduced to few transverse threads that seem to be attached to a thin core filament. The core filament at the right arrow seems to be in continuity with another filament. Bars, 0.01 μm. × 131,600 (a); × 380,500 (*inset*).

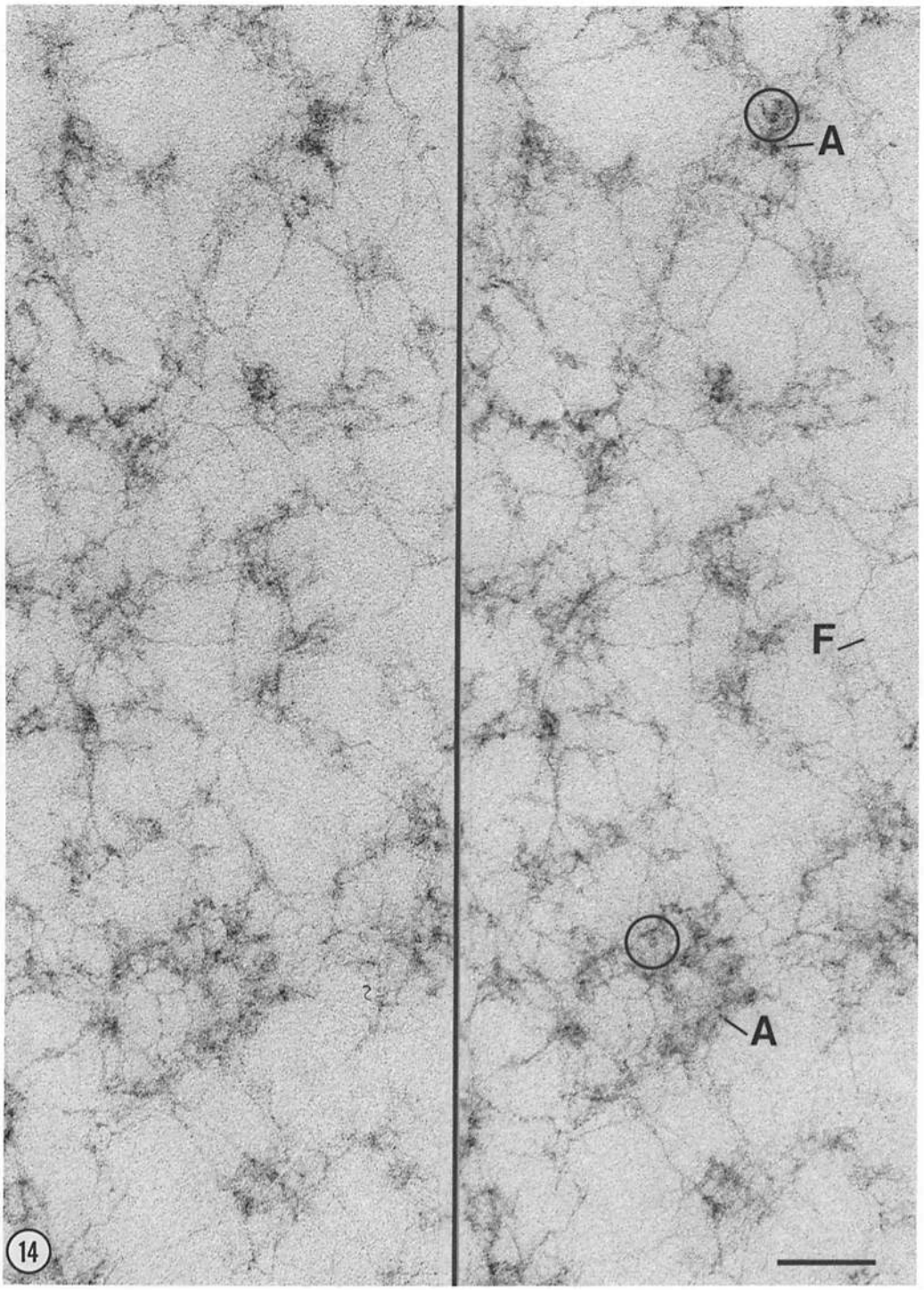

FIGURE 14 Stereo pair of micrographs of Reichert's membrane treated by plasmin for 2 h. The network of fine filaments (*F*) extends in three dimensions. Cross sections of basotubules (circles) may be distinguished within the islands of electron dense, amorphous material (*A*). Bar, 0.1 μm. × 145,000.

dimensions, the junction of the filaments can occasionally be observed in detail, particularly in 2-nm thick sections. Thus, the junction shown as an "H" pattern at the arrow in Fig. 15 consists of two upper filaments united by a short vertical span with the two lower filaments. The connecting span could appear thick (Fig. 16*a*) or double (Fig. 16*b*) and was ~30-nm long (Fig. 16*a*).

At an early stage of plasmin digestion, the filaments show 3–4 nm dots (Fig. 13) that at high magnification may be resolved into pairs (Fig. 17, *a* and *b*). However, in the areas where digestion is advanced, dots disappear (Fig. 14) and the abundance of filaments may be reduced. To measure the distance between dots, two weakly digested areas were selected; and the dots were enumerated along filament lengths of 27.8 μm and 10.3 μm, respectively, as measured in a Zeiss MOP. Dividing the filament length by the number of dots encountered gave the mean interdot distance, 819 nm in the first area and 859 nm in the second.

When the plasmin treatment is prolonged for 15, 24, or 48 h, the filaments are no longer recognizable and, presumably, have been digested away.

BASOTUBULES: After a 2-h plasmin treatment, the filamentous network is associated with islands of electron-dense material, within which basotubules seem to be preferentially

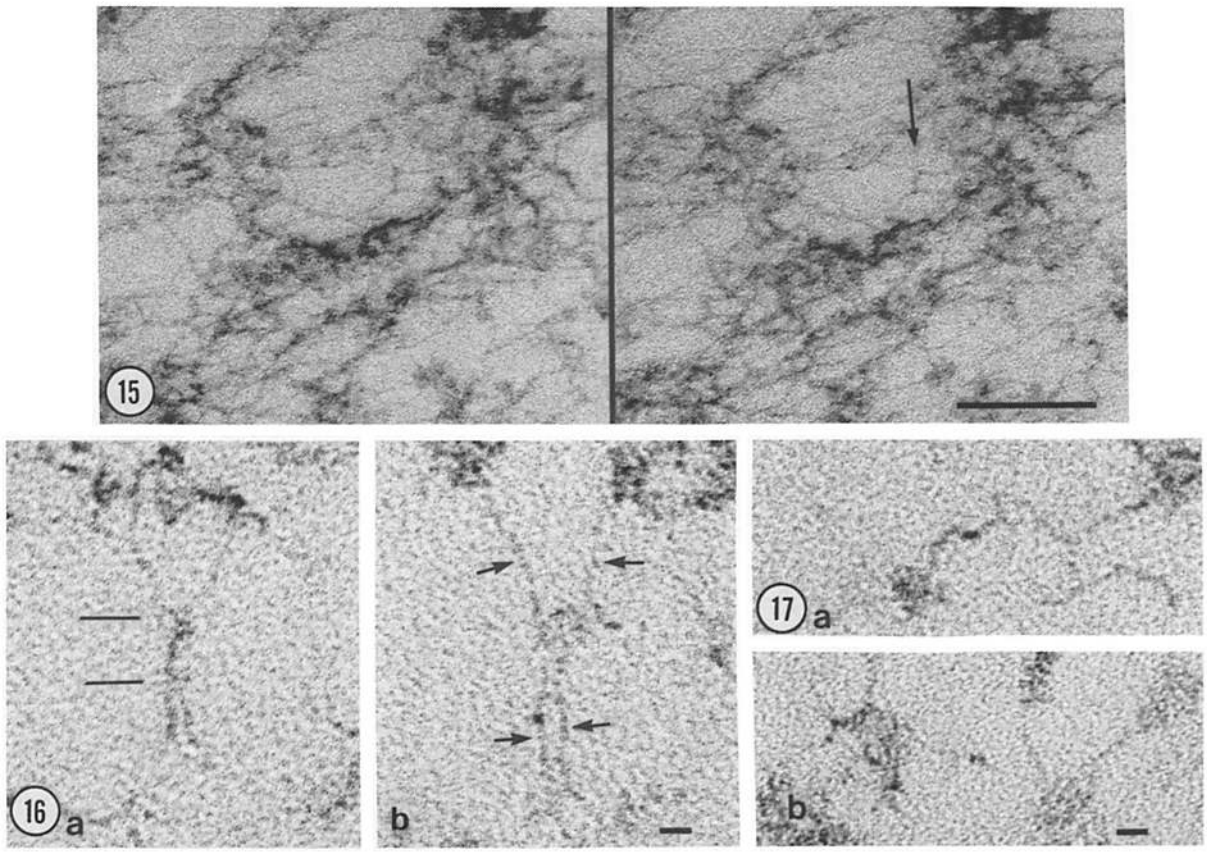

FIGURES 15–17 Structural features of fine filaments observed in 2 h plasmin-digested Reichert's membrane. Fig. 15: Stereo-electron micrographs in which the arrow points to an H pattern, that is, a short vertical span connecting an upper pair and a lower pair of joining filaments. Bar, 0.1 μm. × 183,000. Fig. 16: Higher power views of similar spanned structures. In *a*, the upper and lower pairs of joining filaments are united by a thick, 30-nm long span (demarcated by two horizontal lines). In *b*, the paired filaments (arrows) are united by a double span. Bar, 0.01 μm. × 375,800. Fig. 17: At high magnification the dots observed along filaments in plasmin treated preparations may be resolved into pairs as seen in the center of the two pictures. Each member of the pair measures ~3 nm and is connected to a single filament. Bar, 0.01 μm. × 375,800.

located (Fig. 14).

When the plasmin treatment is extended to 15 h, the disappearance of the filamentous network facilitates the identification of basotubules. They are surrounded by dense material that is similar to the peritubular feltwork observed after permanganate fixation, as shown in Fig. 18 where two basotubules appear at medium magnification as straight rods within some peritubular feltwork and in Fig. 19 where, at higher magnification, the basotubules present an electron-lucent lumen and the feltwork may be seen in some detail.

In places, the peritubular feltwork is digested away. A ribbon-like helical material then appears at the surface of basotubules (Fig. 20 *b*). Initially, this material consists of a 6-nm wide ribbon that is tightly wound at the surface of the tubule proper, but loosens and enlarges under plasmin influence (Fig. 21, *a–c*). This ribbon, referred to as "helical wrapping," may eventually be freed from the tubule (Fig. 21 *a*). Tubules without helical wrapping lose their straightness and may appear wavy (Fig. 20). Furthermore, their wall is less distinct and, in longitudinal sections, may show a series of electron-dense lines (Fig. 22 *a*) that we interpret as indicating that the tubules are breaking up into disk-like units (Fig. 22 *b*); these units in face view appear as pentagons centered by a dot (Fig. 22, *c* and *d*).

Exposure of Reichert's membrane to plasmin for periods as long as 24 or 48 h leads to disappearance of the basotubules.

DOUBLE PEG: After 48 h of plasmin digestion, no structures are recognizable except for the minute elements described as "double pegs." They are arranged in linear fashion (Fig. 23 *a*), being separated from one another by an interval of ~10 nm (Fig. 23 *b*). As in the intact Reichert's membrane, they appear at high magnification as pairs of minute rods (Fig. 23 *c*) and their linear arrangement is interpreted as the result of interconnection by a fine filament measuring ~1 nm in diameter (Fig. 23 *d*).

Immunostaining

ANTILAMININ ANTIBODIES: After incubation of Reichert's membrane with antilaminin antibodies followed by the peroxidase-antiperoxidase procedure, intense immunostaining is observed along the layers of Reichert's membrane, while the interlayer spaces are barely or not at all stained (Fig. 24). At high magnification, the immunostaining may be assigned to cord-like structures ~10–13-nm thick and separated by lighter spaces (Fig. 25).

ANTITYPE IV COLLAGEN ANTIBODIES: After a 2-h incubation in plasmin, the digested regions immunostained for type IV collagen show a distribution of reaction product along faint lines interconnected into a network pattern (Fig. 26).

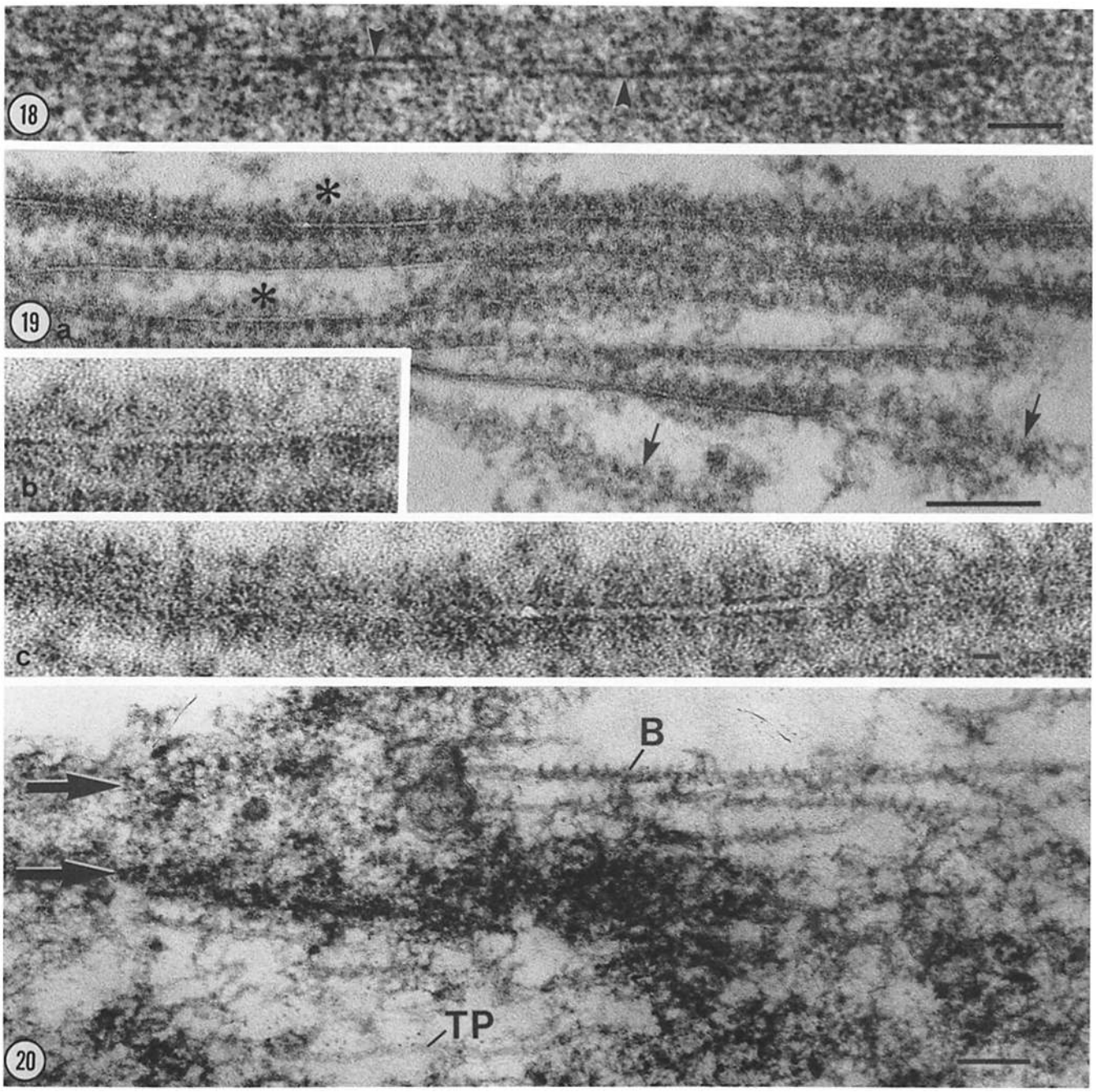

FIGURES 18–20 Longitudinally sectioned basotubules in Reichert's membranes treated with plasmin for 15 h and fixed in glutaraldehyde. Fig. 18: Two basotubules are present (arrowheads) which, at the magnification used, appear as dark rods. They are surrounded by peritubular feltwork. Bar, 0.1 μm. × 118,700. Fig. 19: Higher power view of several basotubules in which the two walls and a lumen, as well as the peritubular feltwork are visible. *a* shows five longitudinally cut basotubules, while at the arrows, the section cuts through the plane of a peritubular feltwork. *b* and *c* show the areas indicated by asterisks in *a* at higher magnification. Bars, 0.01 μm. × 180,700 (*a*); × 406,100 (*b* and *c*). Fig. 20: A portion of Reichert's membrane in which, at upper left the layer arrangement is barely recognizable (arrows). At upper right and lower left center, advanced digestion has eliminated the layered arrangement and has revealed basotubules devoid of peritubular feltwork. These basotubules may show a loosened helical wrapping (*B*) or appear bare (*TP*). Bar, 0.1 μm. × 116,600.

DISCUSSION

Several components have been identified in Reichert's membrane: (*a*) a network of anastomosing cords that constitutes the bulk of the membrane, (*b*) basotubules that usually run parallel to its surface and are associated with a peritubular feltwork, and (*c*) tiny double pegs distinct from cords and basotubules.

Network of Cords

The three-dimensional web described as a network of cords is densely packed within the layers of Reichert's membrane and more loosely arranged in the lucent spaces between layers. The term cord has been used in preference to fibril (8–14) because it better reflects the uneveness and network arrangement of the structure.

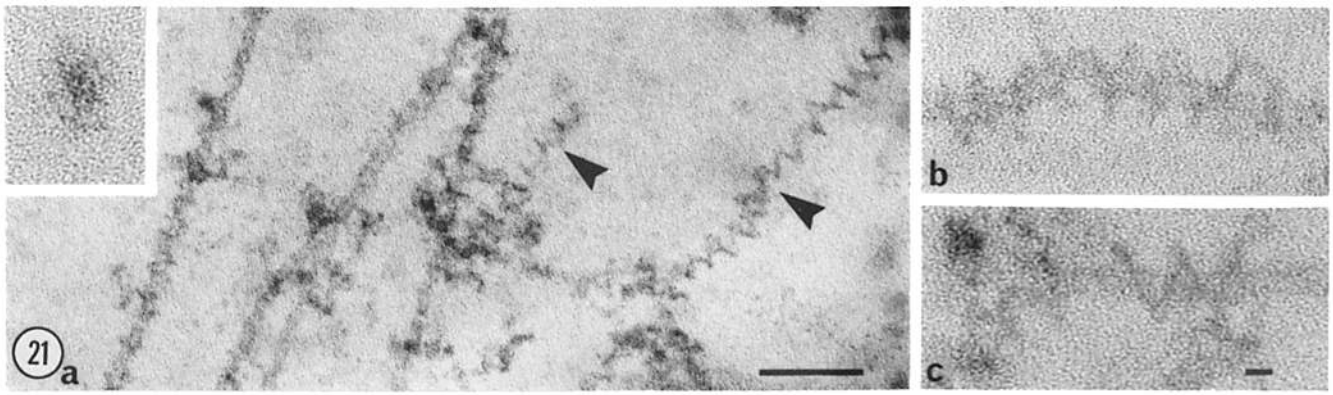

FIGURE 21 Helical wrappings resulting from the action of plasmin on basotubules. *a* shows, at left, basotubules with loosened helical wrappings and, at right, free helical wrappings (arrowheads). Bar, 0.1 μm. × 135,400. In the *inset*, a slightly oblique section of a basotubule is surrounded by a halo interpreted as a loosened helical wrapping. At the same magnification as the *inset*, *b* and *c* show longitudinal sections of basotubules with loosened helical wrapping. Bars, 0.01 μm. × 338,900.

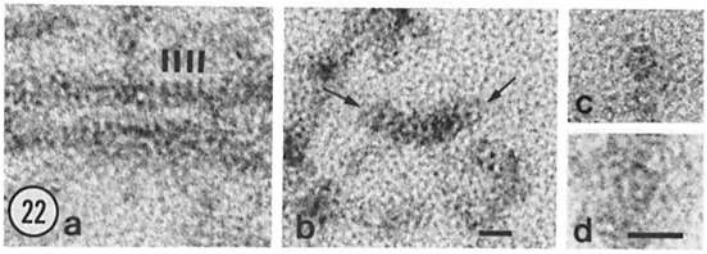

FIGURE 22 Disassembly of basotubules under the influence of plasmin. *a* shows two bare basotubules running across the figure. The short parallel bars point to electron dense bands across the tubule; these are interpreted as indicating that plasmin causes basotubules to split up into disks. *b* shows seven disks overlapping one another (arrows); their central dot is distinguishable. *c* shows a disk seen face on; it appears polygonal. Bar, 0.01 μm. × 434,400. *d* depicts a polygonal disk at a higher magnification. Bar, 0.01 μm. × 729,450.

When Reichert's membrane is treated with the proteolytic enzyme, plasmin, the cords are shown to consist of a sheath that is removed by a short plasmin digestion and a filament that is more resistant to plasmin. Since there is evidence that plasmin preferentially digests laminin and fibronectin (13), these two substances may be present in the sheath. So far, the presence of laminin has been detected by immunostaining. The immunostained material appears as cord-like elements, somewhat thicker than the cords observed under normal conditions, possibly due to stain accumulation at their surface. A 2-h plasmin treatment eliminates the immunostaining from digested areas. It thus appears that a substance with laminin antigenicity, presumably laminin itself, is a component of the cords. Recently, sections of Reichert's membrane embedded in Lowycril (J. B. EM Services, Inc., Montreal) were immunostained for laminin using gold particles as marker; examination of stereopairs revealed that most gold particles overlaid the cords at the surface of the section (unpublished work with D. Grant). It is concluded that laminin is present within the cords of Reichert's membrane.

Digestion of the cord sheath by a 2-h plasmin treatment unveils a filament that in three dimensions forms a continuous network. Under normal conditions, the filament is barely or not at all visible, but it becomes prominent within the cord at an early stage of plasmin digestion. At a later stage, the network of cords is substituted by a network of filaments. Two features occasionally noted along the filaments, a 30-nm span connecting pairs of joining filaments and dots separated by a distance of 819–859 nm, are compatible with the model of type IV collagen network proposed by Timpl et al. (25) on the basis of rotary-shadowing data. According to this model, each type IV collagen molecule is in continuity at one end with another collagen molecule through an 8.6-nm globular domain and, at the other end, with three other molecules associated into a 30-nm long connector known as the "short form of 7S collagen." The distance between two consecutive globular domains is estimated at 800 nm, that is, the length of two type IV collagen molecules (25). The similarities between the features of the model and our measured data raise the possibility that the filamentous network consists of molecules of type IV collagen in continuity. Type IV collagen immunostaining of Reichert's membrane exposed for 2 h to plasmin showed a reaction along the filamentous network. Recent results with D. Grant, using a gold marker on Lowycryl sections, provided further evidence of the presence of type IV collagen within the cords. It is concluded (Fig. 27) that the cords are constituted of a plasmin-extractable sheath containing laminin and of a core filament composed of type IV collagen.

Basotubules

While the existence of basotubules is well established, the peritubular feltwork appearing after permanganate fixation or after a 15-h plasmin treatment is not readily seen after glutaraldehyde fixation of untreated tissue. The possibility has not been eliminated that it is an artefact of fixation resulting from precipitation of nearby cords at the surface of basotubules. However, we are inclined to believe that it is a real structure. Thus, the dense islands observed along the filament network after a 2-h plasmin treatment and glutaraldehyde fixation (Fig. 14) may correspond to the peritubular feltwork.

The basotubules themselves are hollow rods with a diameter of 7–10 nm. They appear as rigid structures that mainly run in the plane of the layers, that is, in parallel with the surface of Reichert's membrane. Basotubules are composed of two

parts illustrated in Fig. 28: (*a*) the tubule proper and (*b*) a flat ribbon ~1-nm thick and 6-nm wide, tightly wound around the surface in the manner of a bandage and referred to as helical wrapping. The cross section of basotubules is generally circular, but tends to appear pentagonal either when the peritubular feltwork is lacking (Fig. 11 *d*) or after long plasmin digestion (Fig. 22, *c* and *d*). In the latter case, we interpret the observations as indicating that the tubule proper is dissociated into more or less pentagonal units with a central dot. The negative staining of an amyloid fraction by Bladen et al. (26) has shown the presence of tubular structures composed of 8.5–9.5-nm wide pentagonal units with a central dot. This material has been later characterized as the "amyloid P component" (27–29). The similarity between these and our observations raises the possibility that the amyloid P component is present within basotubules.

Breathnach et al. (30) have shown that antibodies to the

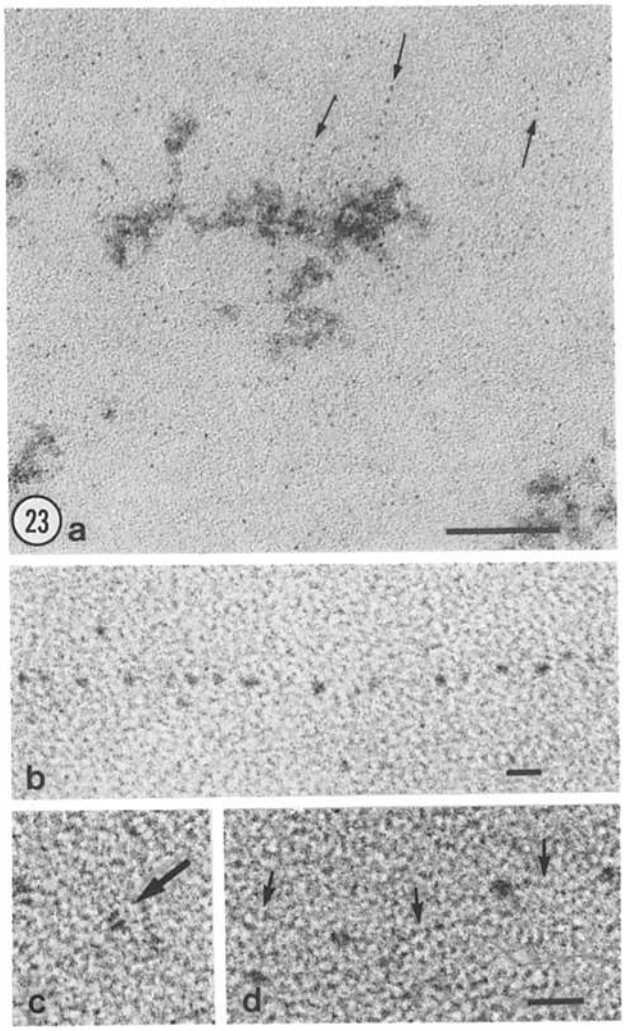

FIGURE 23 Double peg structures observed after a 48-h incubation of Reichert's membrane in plasmin. *a* shows the double pegs as rows of tiny dots often arranged in more or less linear array (arrows). The rows appear free or associated with unidentified remnants. The other components of Reichert's membrane are nearly completely disintegrated. *b* is a high power view of a row of double pegs. *c* and *d* at very high magnification show the double pegs as made up of two short parallel lines (thick arrow in *c*). Moreover, the double pegs are joined by a very fine filament (small arrows in *d*). Bars, 0.01 μm. × 151,900 (*a*); × 430,300 (*b*); × 722,400 (*c* and *d*).

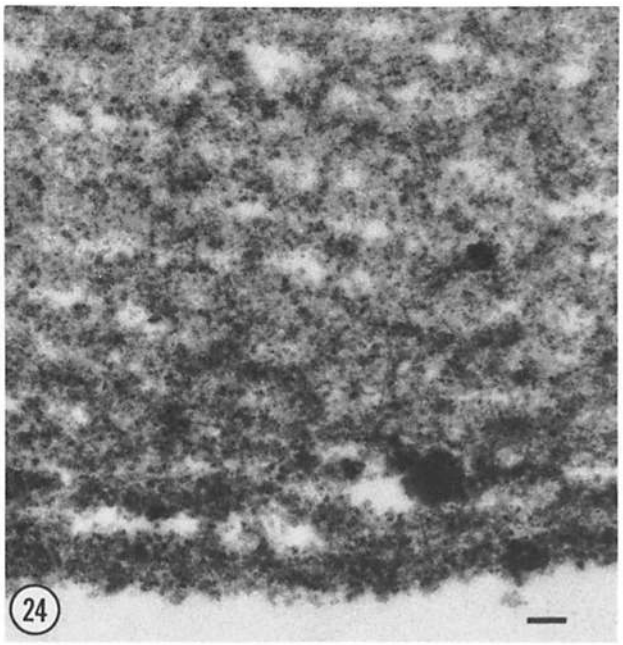

FIGURE 24 Electron micrograph of Reichert's membrane immunostained for laminin. Formaldehyde-fixed slices cut perpendicular to the surface were incubated with antilaminin antibodies, followed by the PAP sequence, DAB-H_2O_2, and osmium tetroxide. The intense immunostaining of Reichert's membrane predominates along the layers. Bar, 0.1 μm. × 51,300.

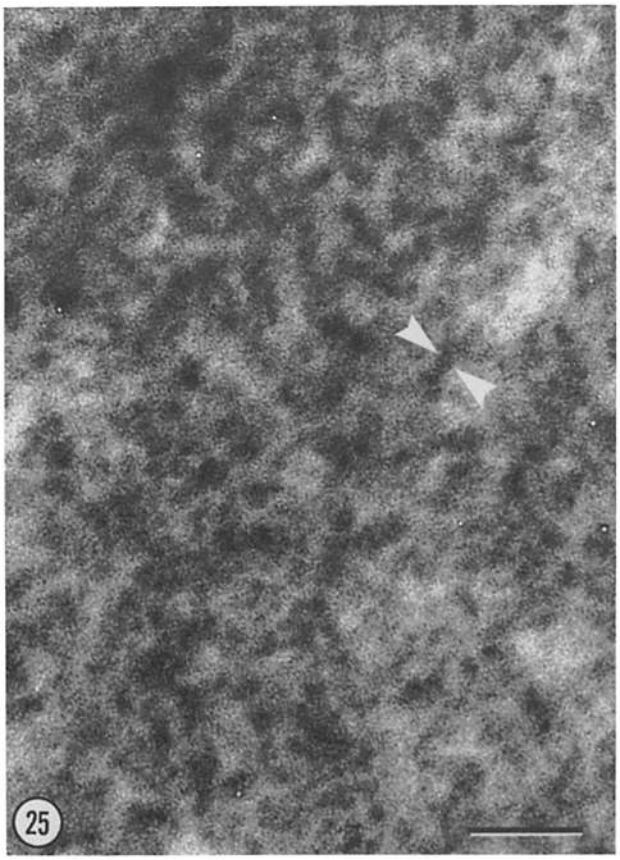

FIGURE 25 Higher magnification view of Reichert's membrane immunostained for laminin as in Fig. 24. Immunostaining of cord-like structures is seen (arrowheads). Bar, 0.1 μm. × 148,600.

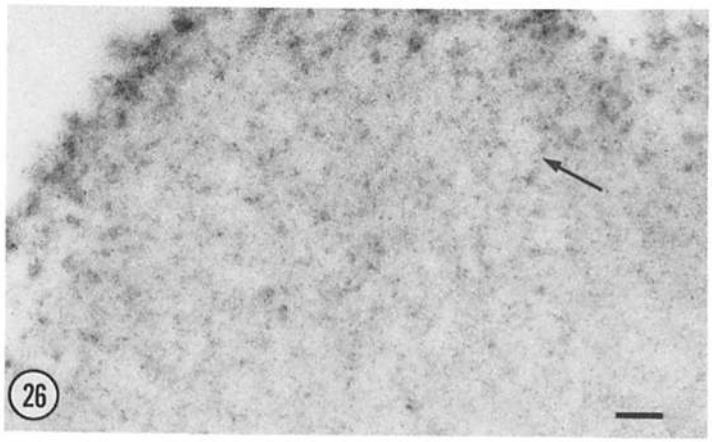

FIGURE 26 Electron micrograph of Reichert's membrane treated with plasmin for 2 h and immunostained for type IV collagen by incubation with peroxidase conjugated antitype IV collagen antibodies followed by DAB-H_2O_2 and osmium tetroxide. A moderate immunostaining is seem as more or less dense reaction product arranged in a network pattern (arrow). Bar, 0.1 μm. × 60,300.

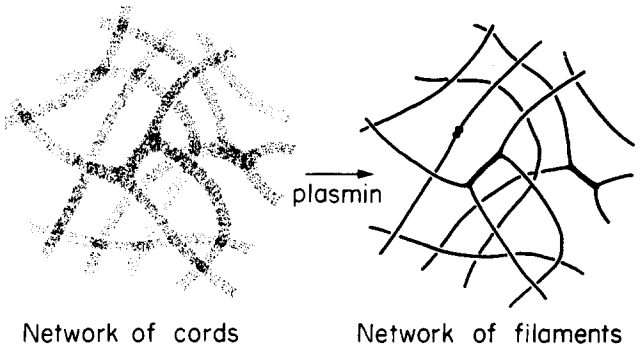

FIGURE 27 The diagram at left represents our interpretation of the network arrangement of the cords within the layers of Reichert's membrane, whereas the diagram at right depicts the effect of a short plasmin treatment. Cords thus appear to be composed of a sheath, which, when gradually digested away by plasmin, reveals the presence of a more plasmin-resistant axial filament. Immunostaining data further indicate that the sheath contains laminin, whereas the filament consists of type IV collagen.

amyloid P component immunostain the microfibrils found at the periphery of elastic fibers. Intimate relation between microfibrils and basement membranes has been reported in the alveolar tissue of the human lung (31, 32), the glomerular capillaries of normal (3, 33–35) and diseased kidney (35–37) and other tissues (32, 38, 39). Kewley et al. (40, 41) have prepared an antiserum against the microfibrillar protein of elastic tissue and found that it immunostained basement membranes in a variety of human tissues including kidney (41)—a result suggesting that basement membranes contain a structure with the same antigenicity as microfibrils. It is tempting to conclude that the microfibril-like material associated with basement membranes is the basotubule. However, the rigid-looking basotubules of Reichert's membranes should not be equated with the flexible-looking microfibrils, such as those seen looping around blobs of elastic tissue. Perhaps basotubules share some, but not all, components with microfibrils. Breathnach et al. (30) have proposed that the amyloid P component is associated with MFP I, one of the two glycoproteins extracted from microfibrils by Sear et al. (42).

In the hope of clarifying the problem we have recently applied an antiserum against mouse amyloid P component (kindly provided by Dr. Martha Skinner, University Hospital, Boston, MA) to the mouse Reichert's membrane; the basotubules have thus been immunostained (Inoué, S., and C. P. Leblond, in preparation). It is concluded that the amyloid P component is a constituent of basotubules.

Double Pegs

Because of the minute size—3.5 nm—of the dot-like structures referred to as double pegs, the question arises as to whether they are artefactual. However, they have been observed not only in intact Reichert's membrane but also after a 48-h plasmin treatment when they become prominent due to degradation of all other structures. Moreover, double pegs have been observed in the glomerular basement membrane of the rat kidney (G. W. Laurie, C. P. Leblond, S. Inoué, G. R. Martin, and A. Chung, in preparation) and they are present in extracts of the mouse EHS tumor (unpublished results). We, therefore, propose that double pegs are a real ultrastructural component of the tissue.

CONCLUDING REMARKS

Reichert's membrane, a multilayered basement membrane, consists of several ultrastructural components. The major constituent is a network of cords averaging 5 nm in width. The network is organized tightly within the layers and loosely in the interlayer spaces. In both, the cords are composed of a type IV collagen filament running within a sheath rich in laminin. The other components of the membrane are rigid-looking basotubules that may impart strength to the layers, and tiny particles referred to as double pegs whose role is unknown.

By immunohistochemical staining, Reichert's membrane has been previously shown to contain not only laminin (14–17, 43) and type IV collagen (18–20), but also heparan sulfate proteoglycan (44), fibronectin (43), and entactin (unpublished results with D. Grant). Since these five substances have also been detected by immunostaining of the glomerular basement membrane in the rat kidney (laminin, reference 45; type IV collagen, reference 45; heparan sulfate proteoglycan, reference 46; fibronectin, reference 45; entactin, Laurie et al., in preparation), we have recently examined whether this basement membrane has an ultrastructure comparable to that of Reichert's membrane. Indeed, cords with a mean diameter of 4 nm are arranged into a tight network within the lamina densa of the glomerular basement membrane and loosely extend across the adjacent laminae lucidae (rarae). Moreover, there are 7–10-nm wide basotubules (previously noted as hollow 10–11-nm wide fibrils; references 3, 4, and 7) and 3.5-nm double pegs strung along fine filaments (Laurie et al., in preparation).

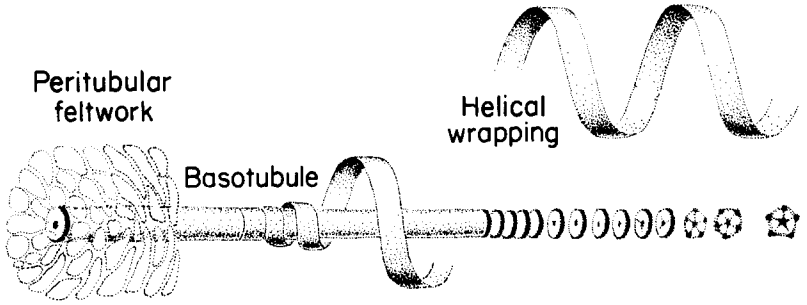

FIGURE 28 Interpretation of basotubule structure. At left, the normal basotubule is surrounded by peritubular feltwork. From left to right, the changes resulting from increasing duration of plasmin treatment are depicted. First, the peritubular feltwork is removed and, as a result, the basotubule is clearly visible. Next, the helical wrapping becomes prominent and loosens, revealing the tubule proper. Finally, the helical wrapping is released, while the tubule proper breaks up into units that tend to take on a pentagonal shape.

These observations suggest that the glomerular basement membrane and perhaps other common basement membranes are composed of the same structural elements as Reichert's membrane.

This investigation was greatly facilitated by the assistance of Dr. L. Liotta who provided purified plasmin and Dr. G. R. Martin who supplied the antibodies to laminin and type IV collagen. The help of Dr. Y. Clermont on revising the manuscript is acknowledged.

This work was supported by grants from the National Institutes of Health (1RO1 DE 0569) and the Medical Research Council of Canada. G. W. Laurie was supported by a National Fellowship Award from the Kidney Foundation of Canada.

The findings have been presented in poster form at the Baltimore meeting of the American Society for Cell Biology in November, 1982 (*J. Cell Biol.* 95:131a).

Received for publication 21 March 1983, and in revised form 22 July 1983.

REFERENCES

1. Kefalides, N. A., R. Alper, and C. C. Clark. 1979. Biochemistry and metabolism of basement membranes. *Int. Rev. Cytol.* 61:167–228.
2. Laurie, G. W., C. P. Leblond, and G. R. Martin. 1982. Localization of type IV collagen, laminin, heparan sulfate proteoglycan, and fibronectin to the basal lamina of basement membranes. *J. Cell Biol.* 95:340–344.
3. Farquhar, M. G., S. L. Wissing, and G. E. Palade. 1961. Glomerular permeability. I. Ferritin transfer across the normal glomerular capillary wall. *J. Exp. Med.* 113:47–66.
4. Latta, H. 1970. The glomerular capillary wall. *J. Ultrastruct. Res.* 32:526–544.
5. Rodewald, R., and M. J. Karnovsky. 1974. Porous substructure of the glomerular slit diaphragm in the rat and mouse. *J. Cell Biol.* 60:423–433.
6. Vaccaro, C. A., and J. S. Brody. 1981. Structural features of alveolar wall basement membrane in the adult rat lung. *J. Cell Biol.* 91:427–437.
7. Farquhar, M. G. 1981. The glomerular basement membrane. A selective macromolecular filter. *In* Cell Biology of Extracellular Matrix. E. D. Hay, editor. Plenum Press, New York. 335–378.
8. Laurie, G. W., and C. P. Leblond. 1982. Intracellular localization of basement membrane precursors in the endodermal cells of the rat parietal yolk sac. I. Ultrastructure and phosphatase activity of endodermal cells. *J. Histochem. Cytochem.* 30:973–982.
9. Clark, C. C., R. R. Minor, T. R. Koszalka, R. L. Brent, and N. A. Kefalides. 1975. The embryonic rat parietal yolk sac. Changes in the morphology and composition of its basement membrane during development. *Dev. Biol.* 46:243–261.
10. Jollie, W. P. 1968. Changes in the fine structure of the parietal yolk sac of the rat placenta with increasing gestational age. *Am. J. Anat.* 122:513–532.
11. Martinez-Hernandez, A., P. K. Nakane, and G. B. Pierce. 1974. Intracellular localization of basement membrane antigen in parietal yolk sac cells. *Am. J. Pathol.* 76:549–559.
12. Wislocki, G. B., and E. W. Dempsey. 1955. Electron microscopy of the placenta of the rat. *Anat. Rec.* 123:33–63.
13. Liotta, L. A., R. H. Goldfarb, R. Brundage, G. P. Siegal, V. Terranova, and S. Garbisa. 1981. Effect of plasmin activator (urokinase), plasmin, and thrombin on glycoprotein and collagenous components of basement membrane. *Cancer Res.* 41:4629–4636.
14. Hogan, B. L. M., A. K. Cooper, and M. Kurkinen. 1979. Incorporation into Reichert's membrane of laminin-like extracellular proteins synthesized by parietal endoderm cells of the mouse embryo. *Dev. Biol.* 80:289–300.
15. Howe, C. C., and D. Solter. 1980. Identification of non-collagenous basement membrane glycopeptides synthesized by mouse parietal endoderm and an entodermal cell line. *Dev. Biol.* 77:480–487.
16. Smith, K. K., and S. Strickland. 1981. Structural components and characteristics of Reichert's membrane, an extra-embryonic basement membrane. *J. Biol. Chem.* 256:4654–4661.
17. Laurie, G. W., C. P. Leblond, G. R. Martin, and M. H. Silver. 1982. Intracellular localization of basement membrane precursors in the endodermal cells of the rat parietal yolk sac. III. Immunostaining for laminin and its precursors. *J. Histochem. Cytochem.* 30:991–998.
18. Adamson, E. D., and S. E. Ayers. 1979. The localization and synthesis of some collagen types in developing mouse embryos. *Cell.* 16:953–965.
19. Tryggvason, K., P. Gehron Robey, and G. R. Martin. 1980. Biosynthesis of type IV procollagens by tumor and parietal yolk sac tissue in mouse. *Biochemistry.* 19:1284–1289.
20. Laurie, G. W., C. P. Leblond, and G. R. Martin. 1982. Intracellular localization of basement membrane precursors in the endodermal cells of the rat parietal yolk sac. II. Immunostaining for type IV collagen and its precursors. *J. Histochem. Cytochem.* 30:983–990.
21. Goldfischer, S., Y. Kress, B. Coltoff-Schiller, and J. Berman. 1981. Primary fixation in osmium-potassium ferrocyanide. *J. Histochem. Cytochem.* 29:1105–1111.
22. Todd, M. E., and M. K. Tokito. 1981. Improved ultrastructural detail in tissues fixed with potassium permanganate. *Stain Technol.* 56:335–342.
23. Minor, R. R., P. S. Hoch, T. R. Koszalka, R. L. Brent, and N. A. Kefalides. 1976. Organ cultures of the embryonic rat parietal yolk sac. I. Morphologic and autoradiographic studies of the deposition of the collagen and noncollagen glycoprotein components of basement membrane. *Dev. Biol.* 48:334–364.
24. Porter, D. G. 1966. Observations on the yolk sac and Reichert's membrane of ectopic mouse embryos. *Anat. Rec.* 154:847–860.
25. Timpl, R., H. Wiedeman, V. Van Delden, H. Furthmayr, and K. Kühn. 1981. A network model for the organization of type IV collagen molecules in basement membranes. *Eur. J. Biochem.* 120:203–211.
26. Bladen, H. A., M. U. Nylen, and G. G. Glenner. 1966. The ultrastructure of human amyloid as revealed by the negative staining technique. *J. Ultrastruct. Res.* 14:449–459.
27. Cathcart, E. S., T. Shirahama, and A. S. Cohen. 1967. Isolation and identification of a plasma component of amyloid. *Biochim. Biophys. Acta.* 147:392–393.
28. Cathcart, E. S., F. A. Wollheim, and A. S. Cohen. 1967. Plasma protein constituents of amyloid fibrils. *J. Immunol.* 99:376–385.
29. Binette, P., M. Binette, and E. Calkins. 1974. The isolation and identification of the P-component of normal human plasma proteins. *Biochem. J.* 143:253–254.
30. Breathnach, S. M., S. M. Melrose, B. Bhogal, F. C. de Beer, R. F. Dyck, G. Tennent, M. M. Black, and M. B. Pepys. 1981. Amyloid P component is located on elastic fiber microfibrils in normal human tissue. *Nature (Lond.).* 293:652–654.
31. Low, F. N. 1961. The extracellular portion of the human blood-air barrier and its relation to tissue space. *Anat. Rec.* 139:105–124.
32. Low, F. N. 1962. Microfibrils, fine filamentous components of the tissue space. *Anat. Rec.* 142:131–137.
33. Farquhar, M. G. 1978. Structure and function of glomerular capillaries. *In* Biology and Chemistry of Basement Membranes. N. A. Kefalides, editor. Academic Press, New York. 43–80.
34. Farquhar, M. G., S. L. Wissig, and G. E. Palade. 1961. Glomerular permeability. I. Ferritin transfer across the normal glomerular capillary wall. *J. Exp. Med.* 113:47–66.
35. Hsu, H.-C., and J. Churg. 1979. Glomerular microfibrils in renal disease: a comparative electron microscopy study. *Kidney Int.* 16:497–504.
36. Hsu, H.-C., Y. Suzuki, J. Churg, and E. Grishman. 1980. Ultrastructure of transplant glomerulopathy. *Histopathology (Oxford).* 4:351–367.
37. Olsen, S. 1979. Pathology of the renal allograft rejection. *Monogr. Pathol.* 20:327–355.
38. Carlson, E. C., R. H. Upson, and D. K. Evans. 1974. The production of extracellular connective tissue fibrils by chick notochordal epithelium in vitro. *Anat. Rec.* 179:361–375.
39. Haust, M. D. 1965. Fine fibrils of extracellular space (microfilaments). Their structure and role in connective tissue organization. *Am. J. Pathol.* 47:1113–1137.
40. Kewley, M. A., F. S. Steven, and G. Williams. 1977. Preparation of a specific antiserum to the microfibrillar protein of elastic tissue. *Immunology.* 32:483–489.
41. Kewley, M. A., F. S. Steven, and G. Williams. 1977. Immunofluorescence studies with a specific antiserum to the microfibrillar protein of elastic fibers. Location in elastic and non-elastic connective tissues. *Immunology.* 33:381–386.
42. Sear, C. H. J., M. E. Grant, and D. S. Jackson. 1981. The nature of the microfibrillar glycoproteins of elastic fibers. A biosynthetic study. *Biochem. J.* 194:587–598.
43. Amenta, P. S., C. C. Clark, and A. Martinez-Hernandez. 1983. Deposition of laminin and fibronectin in the basement membrane of the rat parietal yolk sac. *J. Cell Biol.* 96:104–111.
44. Hogan, B. L. M., A. Taylor, and A. R. Cooper. 1982. Murine parietal endodermal cells synthesize heparan sulfate and 170 K and 145 K sulfated glycoproteins as components of Reichert's membrane. *Dev. Biol.* 90:210–214.
45. Courtoy, P. J., R. Timpl, and M. G. Farquhar. 1982. Comparative distribution of laminin, type IV collagen and fibronectin in the rat glomerulus. *J. Histochem. Cytochem.* 30:874–886.
46. Kanwar, Y. S., and M. G. Farquhar. 1981. Presence of heparan sulfate in the glomerular basement membrane. *Proc. Natl. Acad. Sci. USA.* 76:1303–1307.